EUROfusion

WPJET2-PR(18) 20724

J Holgate et al.

Rotational breakup of metal droplets in tokamak edge plasmas

Preprint of Paper to be submitted for publication in
Physical Review Letters

This work has been carried out within the framework of the EUROfusion Consortium and has received funding from the Euratom research and training programme 2014-2018 under grant agreement No 633053. The views and opinions expressed herein do not necessarily reflect those of the European Commission.

Rotational breakup of metal droplets in tokamak edge plasmas

J. T. Holgate,[1,2] L. Simons,[1,2,a)] Y. Andrew,[1,2] C. K. Stavrou,[2,3] and JET Contributors[b)]
[1)] *Blackett Laboratory, Imperial College London, London, SW7 2BW, UK*
[2)] *Culham Centre for Fusion Energy, Culham Science Centre, Abingdon, Oxfordshire, OX14 3DB, UK*
[3)] *Aalto University, Department of Applied Physics, Espoo, Finland*

(Dated: 9 July 2018)

Observations of branched tracks with fast cameras in tokamaks are presented and explained using a theoretical model of the rotational breakup of molten metal droplets. Simulations performed with the dust tracking code DTOKS produce visibly similar droplet trajectories with breakup timescales in agreement with camera diagnostics. The breakup of these droplets suggests rotational velocities in excess of 10^5 s^{-1}, two orders of magnitude greater than previous measurements of macroparticles spinning in plasmas. The rotational breakup of tungsten droplets is beneficial for the operation of future fusion devices; predictions for the International Thermonuclear Experimental Reactor (ITER) suggest that higher magnetic fields, plasma temperatures and plasma densities will enhance the breakup process, thus protecting the core plasma from acute impurity deposition and subsequent disruption events.

Keywords: Fusion, tokamaks, dusty plasmas, rotation, disruption mitigation

The generation of energy through fusion has been a longstanding goal of physicists since Eddington's original hypothesis of nuclear fusion as the origin of stellar energy, and prediction of its terrestrial uses, nearly a century ago[1]. The principal obstacle to fusion power generation is the need to confine hydrogen at sufficient densities and temperatures, for a long enough time, in a steady state[2]. The high-temperature fuel is ionised forming a plasma which must be maintained in a controlled manner to extract energy. The leading device utilising magnetic fields to shape and limit particle transport to the plasma facing surfaces (PFCs), is the tokamak. The research and development effort towards a demonstration power plant (DEMO) has highlighted the need for progress in diagnosis and control of plasma and divertor design to ensure optimised fusion power performance[3]. Tungsten is the preferred material for the first wall for current and next-generation tokamaks, due to its high melting point and low chemical reactivity[4,5]. In spite of this, interaction of the plasma with the PFCs causes surface erosion by physical and chemical sputtering, where individual atoms are removed from the surface[6], and melting either through bulk melting due to high heat fluxes from the plasma[7] or local melting caused by unipolar arcs[8] and micro-exposed cracked surfaces[9]. The various melting and erosion mechanisms inject 1–100 μm-scale liquid drops into the tokamak[10]. The high atomic mass of tungsten causes strong bremsstrahlung radiation losses, which inhibit the successful operation of a fusion device; the maximum tolerable concentration of tungsten impurities is of the order of 10^{-5} tungsten atoms per hydrogen atom[11,12]. Exceeding this can lead to departure from high-confinement modes of operation[13] or the complete loss of plasma stability and termination of the discharge in a disruption[14]. Disruptions are highly damaging to the tokamak vessel and must be minimized; radiative collapse due to impurities is the leading cause of disruptions in current machines[14]. It is, therefore, imperative to keep tungsten impurities in the confined plasma to a minimum. Understanding and exploiting mechanisms triggering the disintegration of liquid impurities in the divertor region is therefore vital for recycling as well as stable operation of tokamaks.

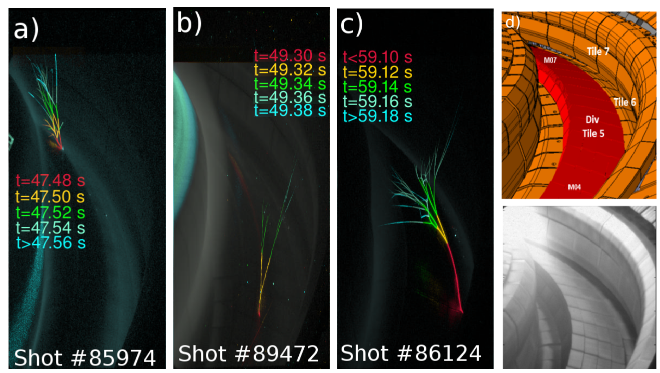

FIG. 1. Breakup of particles observed in JET. (a-c) examples of branched droplet tracks observed with the divertor view camera, colour coded to indicate the time of superimposed frames relative to the start of the pulse. (d) The near infrared view divertor camera.

The presence of liquid metal droplets in tokamaks can be inferred from the large quantities of spherical particles, hollow spheres formed from molten flakes and resolidified liquid beryllium marks which have been collected from the interiors of the vessels of various machines[15–18]. Though previously molten tungsten spheres are not observed in JET, it is worth noting that no dust at all has been recovered from tile 5 in contrast to camera observations, see figure 1(a-c). Understanding the motion and lifetime of these drops is essential in order to determine the quantity and location of impurities they release in the plasma or redeposit on sensitive surfaces such as diagnostic mirrors[21]. One key challenge is to explain the breakup

[a)]Electronic mail: ls5115@ic.ac.uk
[b)]See the author list of "X. Litaudon et al. 2017 Nucl. Fusion 57 102001"

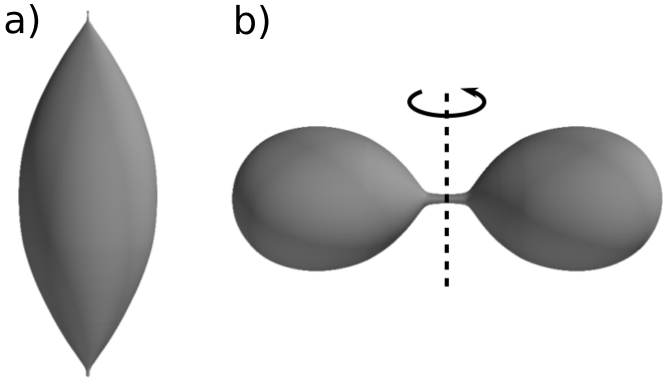

FIG. 2. The shapes of unstable droplets immediately before disruption due to (a) excess charge or (b) rotation. Charged droplets break up by forming two conical tips from which fine jets of subdroplets are ejected. Rotation causes two-lobed break up into a pair of equally-sized droplets. Reproduced with permission from Ref. 33.

of droplets which is observed by fast cameras on tokamaks. Figure 1 shows some characteristic forked trajectories observed in the Joint European Torus (JET) which enter the plasma from the lower divertor region. Similar tree-like trajectories have previously been observed on DIII-D (Ref. 22, Fig. 10) which prompted, in a major review of dust in tokamaks, the remark: "it is unclear what the dust characteristics were and what mechanism was responsible for the observed dust behavior. Further studies are required to clarify this issue" (Ref. 23, p. 31). The present letter answers this outstanding question by considering the rotational breakup of droplets and discusses a beneficial method of limiting impurity transport for future devices such as ITER and DEMO.

Another motivation for studying the spinning of macroscopic particles in plasmas exists in astronomy. The alignment of nonspherical dust grains with the magnetic field in interstellar plasmas leads to the polarization of starlight, discovered nearly 70 years ago by Hall[24] and Hiltner[25], which provides a unique method for measuring the magnetic field of the interstellar medium[26,27]. However, the reliable interpretation of this data depends on a thorough, and elusive, understanding of the mechanism behind dust grain alignment relative to the magnetic field. The leading theory of radiative alignment torque[28,29] describes spinning dust grains which acquire a magnetic moment through the Barnett effect[30]. The interaction between this magnetic moment and the background plasma causes Larmor precession and alignment of the nonspherical dust around the magnetic field. The presence of microscopic rotating charged spheres are also commonly used to explain the anomalous microwave emission from molecular clouds[19,20]. The evidence for rapidly rotating droplets in magnetized tokamak plasmas, as presented in the present paper, could have implications for understanding the alignment of dust grains and the measurement of interstellar magnetic fields or provide an experimental platform for direct measurements of phenomena related to spinning dust in plasmas.

Numerous processes have been proposed for macroparticle spinning in a plasma: examples include the shear of plasma flow[37], asymmetry of radiation to the grain[38], rocket forces from dust grain ablation[39] and the interaction between electric fields and an electrically insulating grain with a dipole caused by plasma flows[40]. The latter process occurs in the plasma sheath, and has been predicted to cause particles to spin at up to 6×10^5 s^{-1} in a low-temperature argon plasma[40]. Other spinning mechanisms relevant to magnetized plasmas include torques generated by $\underline{E} \times \underline{B}$ plasma flows[41], collection of gyrating electrons[30] and ions[42], and a $\underline{J} \times \underline{B}$ Lorentz force from currents flowing through the grain[42]. These spinning mechanisms in scrape off layer plasmas can lead to droplets rotating at $\sim 10^9$ s^{-1} under tokamak conditions[42].

One possible theoretical candidate for explaining the breakup of droplets in tokamaks is electrostatic disruption due to charge accumulation from plasma particle collection. If the internal electrostatic repulsion exceeds the surface tension of the fluid, it becomes unstable. This process leads to a lower limit on droplet size below which they are completely destroyed through a cycle of rapid recharging and breakup[31]. This only occurs for extremely small (10–100 nm) droplets and suggests vaporisation on a timescale of $\sim 10^{-9}$ s once the process has begun. The simulated shape of an unstable charged droplet is displayed in the Fig. 2a; the droplet elongates to form two conical tips from which jets of subdroplets are ejected in accordance with experimental observation[32]. The disruption dynamics and timescales of charged droplets however is inconsistent with the forked trajectories observed in tokamaks.

An alternative mechanism for droplet disintegration is rotational breakup. Rapidly-spinning droplets undergo a two-lobed fissioning process into two equally-sized droplets as illustrated in Fig. 2b leaving with oppositely directed velocities in the centre of mass frame. The scaling of this mechanism is approached through the dimensionless angular velocity which is, according to Chandrasekhar's original definition[35],

$$\Omega = \left(\frac{\rho_d a^3}{8\gamma}\right)^{1/2} \omega_d, \tag{1}$$

where ρ_d, a, γ and ω_d are the density, radius, surface tension and dimensional angular velocity of the droplet, respectively. The maximum value of the dimensionless angular velocity of a stable droplet is $\Omega^* = 0.56$ as verified by theory[35], simulation[36] and experiment[34]. The dimensional angular velocity required to disrupt a 10 μm tungsten droplet, with surface tension 2.5 N m^{-1} and density 17600 kg m^{-3}, is 6×10^5 s^{-1}.

To be in the liquid state, the temperature of a tungsten droplet must exceed 3500 K. At this temperature it emits a large thermal current of electrons which is balanced by the collection of electrons from the plasma[46]. It is assumed that these two currents dominate the charging of the droplet so the collection of ions can be neglected. Each electron striking the droplet provides it with a small additional amount of angular momentum on the order of

$$\Delta L \sim a^2 m_e \left(\omega_{ge} - \omega_d\right), \tag{2}$$

where m_e is the mass of the electron and the electron gyrofrequency is $\omega_{ge} = eB/m_e$. The contribution to the angular momentum of the droplet depends on the difference between the rotational velocity of the electron and the droplet. The flux of electrons to the grain is roughly $\Gamma \sim n_0 v_{te}$ so the approximate torque due to the collection of gyrating electrons is

$$\tau \sim a^2 \Gamma \Delta L \sim a^4 m_e n_0 v_{te} \left(\omega_{ge} - \omega_d\right). \tag{3}$$

Estimating the moment of inertia of the droplet as $\sim \rho_d a^5$ gives the rate of increase in droplet angular velocity,

$$\frac{d\omega_d}{dt} \sim \frac{n_0 v_{te} m_e}{\rho_d a} \left(\omega_{ge} - \omega_d\right). \tag{4}$$

This equation suggests that for an isothermal plasma the droplets will attain the same angular velocity as the electron gyrofrequency which is over 10^{11} s^{-1} for a JET-like magnetic field of $B = 3$ T. However it would take a characteristic spin-up time on the order of $t_{spin} \sim \rho_d a / n_0 v_{ti} m_i$ for the droplet to reach such high values which is roughly 1000 s for 10 μm tungsten droplets under JET-like plasma conditions. This is far longer than the typical survival times of ~ 0.1 s for droplets observed with fast cameras in JET. Solving Eq. 4 for an initially-stationary droplet, and linearizing for $t \ll t_{spin}$, gives an estimate of the angular velocity of a droplet as,

$$\omega_d \sim \frac{m_e v_{te} \omega_{ge}}{m_i v_{ti}} \left[1 - \exp\left(-\frac{m_i n_0 v_{ti}}{\rho_d a} t\right)\right] \tag{5}$$

$$\omega_d \sim \frac{eBn_0 v_{te}}{\rho_d a} t. \tag{6}$$

The corresponding time taken for a droplet in a tokamak to reach the rotational stability limit, $\Omega^* = 0.56$, is

$$t^* \sim \frac{0.56}{eBn_0 v_{te}} \left(\frac{8\gamma\rho_d}{a}\right)^{1/2}. \tag{7}$$

This breakup timescale is plotted in Fig. 3 for tungsten droplets in the edge plasmas of JET and ITER, with magnetic fields of 3 T and 5 T respectively, using typical scrape-off-layer plasma parameters as specified by Tables 2 & 3 of Ref. 49. This is compared with the range timescales of fifteen breakup events observed and recovered dust grain sizes in JET. This plot indicates that tungsten droplets with sizes $a \sim 10$ μm survive for around $t \sim 0.01$ s in JET before they split into a pair of subdroplets due to rotational disruption.

These timescales agree with those of the forked trajectories seen in JET as indicated by Fig. 1(a-c), even despite the rather unrefined estimations used to obtain Eq. 6, suggesting that rotational breakup is a viable explanation of these forked trajectories.

The effect of varying plasma conditions was investigated by introducing rotational breakup into the existing Dust in Tokamaks (DTOKS) particle tracking code. DTOKS[21,48] tracks the motion of dust or droplets by self-consistently solving a charging equation, equation

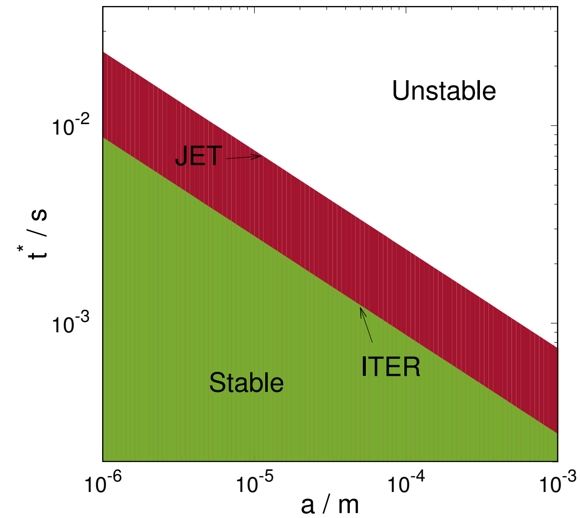

FIG. 3. Estimates of the lifetime of tungsten droplets in JET and ITER like tokamak edge plasmas at different droplet radii and constant plasma conditions.

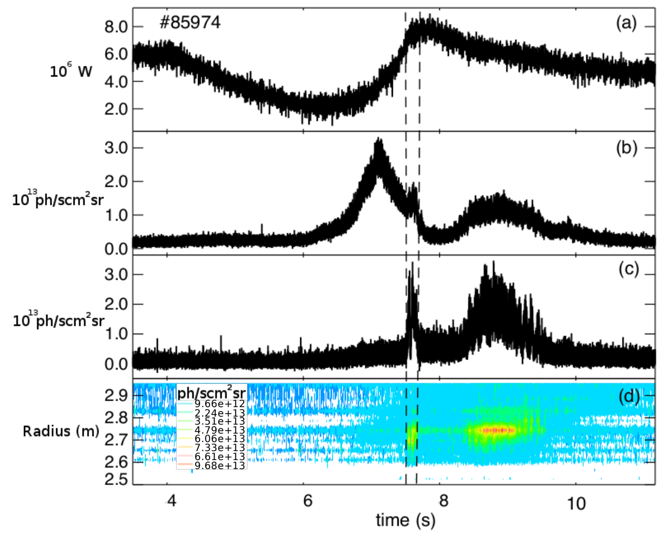

FIG. 4. Total radiated power as measured by vertical viewing bolometer (a), spectroscopy of beryllium 527nm line (b) and tungsten 401nm line (c) and 2d tungsten intensity for shot #85974. A sharp peak in (c) is observed at t=7.5 s at a major radius r=2.7m corresponding to the tracks.

of motion and heating equation as the particle moves through a fixed background plasma which is generated by the EDGE2D/EIRENE code[50]. Recent updates to DTOKS have introduced both electrostatic and rotational breakup mechanisms. The angular velocity of each droplet is calculated, according to Eq. 4, and compared with the $\Omega^* = 0.56$ condition in order to determine the rotational stability of the droplet. The pair of equally-sized subdroplets formed by a rotational breakup event each gain equal and opposite velocities of magnitude $a\omega_d$ in a random orientation which is perpendicular to the magnetic field in the centre of mass frame. The angular momentum of each new droplet is then reset to zero and

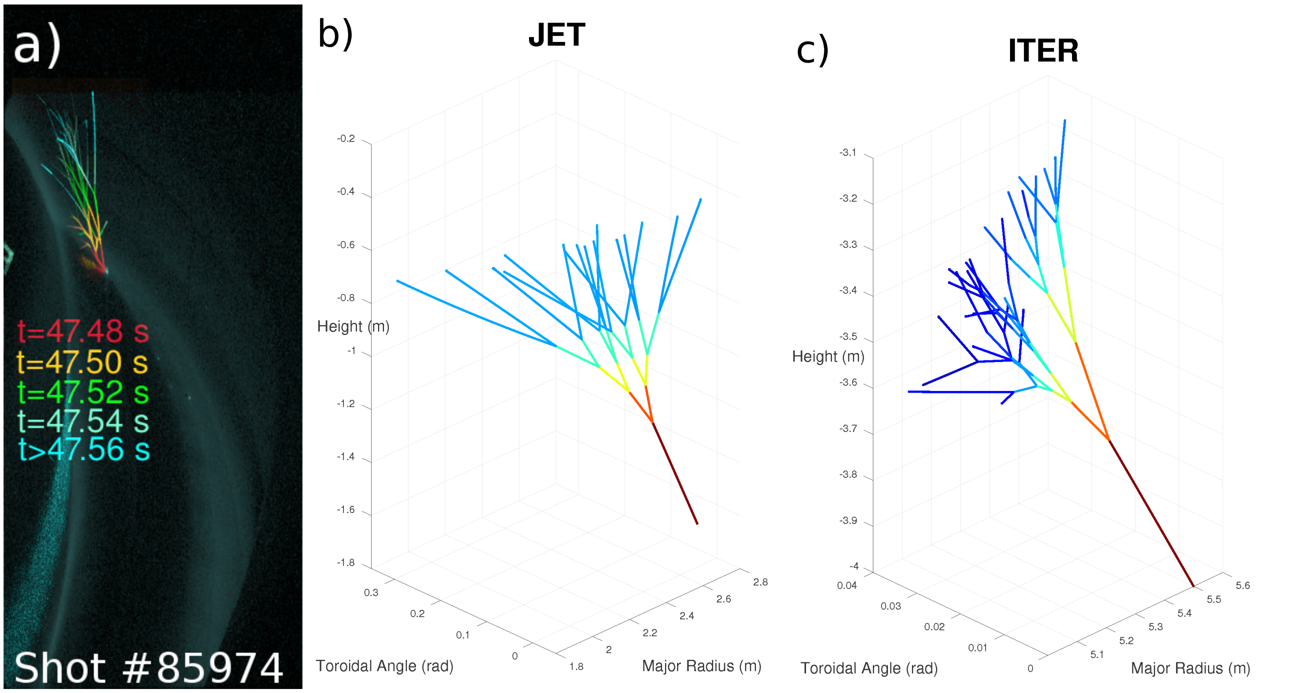

FIG. 5. (a) Reproduction of the branching droplet trajectory from JET pulse number 85974 as captured by the divertor view fast camera. Simulations of tungsten droplet trajectories in JET (b) and ITER (c) with initial radii of 50 μm and temperature $T_d = 3500K$. The plasma background is generated by a EDGE2D simulation using measured parameters from shot 85974 with a magnetic grid retreived from 90414.

their motion is tracked in the same way as for the original droplet.

Simulations by DTOKS have been made for direct comparison with experimental observations on JET. Figure 4 shows a tungsten impurity event at 7.5 s after plasma initiation occuring at the radial coordinate 2.7m. This is evidenced by the measured tungsten intensity 4(c) which is not mirrored in the beryllium spectroscopic signal 4(b). The hot spot from which the tracks originate is measured at a tokamak coordinate (R,Z)=(2.7,-1.6)m. Bolometry measurements in figure 4(a) show no significant change during or immediately after the spectroscopic measurement, consistent with breakup in the scrape off layer. This event is simulated by taking a 50 μm tungsten droplet which is initially at the same location at the corner of tile 5 in the liquid state at its melting temperature of 3500 K and moving with a velocity of (-20,10,50) m s^{-1}. Trajectories terminate either due to electrostatic breakup, escaping the simulation domain or falling below the lower mass limit.

The upgraded DTOKS code produces trajectories as displayed in Fig. 5(b) & 5(c) for JET and ITER plasmas. The simulated trajectory in JET is in good qualitative agreement with that observed with fast cameras in tokamaks, of Fig. 5(a). Note that the smaller droplets near the core might be expected to break up less frequently, according to Eq. 7, but the increase in plasma density and temperature as it approaches the last closed flux surface over-compensates for this effect.

The time taken for this breakup process to occur was measured for each particle. The longest lifetime was $t_{max} = 8.2ms$ with a mean value of $\langle t \rangle = 4.8ms$. Meanwhile for ITER, lifetimes were shorter with $t_{max} = 6.1ms$ and a mean value of $\langle t \rangle = 2.2ms$. The survival times drop sharply as the droplets approach the confined plasma. This pronounced reduction in droplet lifetime is beneficial for future tokamaks as the hazards of tungsten impurities are mitigated by the breakdown of droplets into numerous small droplets which are dispersed over a larger volume of plasma further from the core.

In summary, observations of branching tracks in tokamaks are best explained by considering the rotational stability of molten metal droplets. These droplets collect angular momentum from gyrating electrons in the surrounding plasma and subsequently split into pairs of equally-sized droplets when a critical angular velocity of approximately 10^5 s^{-1} (for 10 μm tungsten droplets) is exceeded. This angular velocity is at least two orders of magnitude greater than any previously-reported observations of macroparticle spinning in plasmas.

The rotational breakup mechanism has been incorporated into simulations of droplet transport in tokamaks and the branched trajectories observed in current-generation tokamaks are well reproduced. Predictive simulations of tungsten droplets in ITER show a large increase in the spinning and disruption rates of droplets compared to the current-generation tokamaks. The enhanced dispersion of small tungsten droplets will mitigate the significant disruption hazard posed by the local deposition of large amounts of tungsten impurities in the core plasma of ITER. As such, the rotational breakup mechanism identified will be highly beneficial to the successful operation of future fusion devices.

We would like to extend our gratitude to our supervisor, Dr. Michael Coppins, and Prof. John Allen for their insights and support. This work has been carried out within the framework of the EUROfusion Consortium and has received funding from the Euratom research and training programme 2014-2018 under grant agreement No 633053. The views and opinions expressed herein do not necessarily reflect those of the European Commission. This work has been supported by the UK's Engineering and Physical Sciences Research Council.

[1] A. S. Eddington *Nature* **106**, 14 (1920).
[2] J. D. Lawson *Proc. Phys. Soc. Sect. B* **70**, 6 (1957).
[3] G. Federici, C. Bachmann, W. Biel, L. Boccaccini, F. Cismondi, S. Ciattaglia, M. Coleman, C. Day, E. Diegele, T. Franke, M. Grattarola, H. Hurzlmeier, A. Ibarra, A. Loving, F. Maviglia, B. Meszaros, C. Morlock, M. Rieth, M. Shannon, N. Taylor, M. Q. Tran, J. H. You, R. Wenninger, and L. Zani, *Fusion Eng. Des.* **109111**, 1464 (2016).
[4] R. Pitts, S. Carpentier, F. Escourbiac, T. Hirai, V. Komarov, A. Kukushkin, S. Lisgo, A. Loarte, M. Merola, R. Mitteau et al. *J. Nucl. Mater.* **415**, S957 (2011).
[5] G. Matthews, M. Beurskens, S. Brezinsek, M. Groth, E. Joffrin, A. Loving, M. Kear, M. Mayoral, R. Neu, P. Prior et al. *Phys. Scr.* **T145**, 014001 (2011).
[6] C. Guillemaut, A. Jardin, J. Horacek, I. Borodkina, A. Autricque, G. Arnoux, J. Boom, S. Brezinsek, J. Coenen, E. De La Luna et al. *Phys. Scr.* **T167**, 014005 (2016).
[7] G. Matthews, B. Bazylev, A. Baron-Wiechec, J. Coenen, K. Heinola, V. Kiptily, H. Maier, C. Reux, V. Riccardo, F. Rimini et al. *Phys. Scr.* **T167**, 014070 (2016).
[8] M. Laux, M. Balden and P. Siemroth, *Phys. Scr.* **T159**, 014026 (2014).
[9] T. Loewenhoff, J. Linke, G. Pintsuk and C. Thomser *Fus. Eng. Des.* **87**, 1201 (2012).
[10] J. W. Coenen, G. Arnoux, B. Bazylev, G. F. Matthews, A. Autricque, I. Balboa, M. Clever, R. Dejarnac, I. Coffey, Y. Corre, S. Devaux, L. Frassinetti, E. Gauthier, J. Horacek, S. Jachmich, M. Komm, M. Knaup, K. Krieger, S. Marsen, A. Meigs, P. Mertens, R. A. Pitts, T. Puetterich, M. Rack, M. Stamp, G. Sergienko, P. Tamain, and V. Thompson, *Nucl. Fusion* **55**, (2015).
[11] A. Kallenbach, R. Neu, R. Dux, H. Fahrbach, J. Fuchs, L. Giannone, O. Gruber, A. Herrmann, P. Lang, B. Lipschultz et al. *Plasma Phys. Control. Fusion* **47**, B207 (2005).
[12] G. Hogeweij, V. Leonov, J. Schweinzer, A. Sips, C. Angioni, G. Calabrò, R. Dux, A. Kallenbach, E. Lerche, C. Maggi et al. *Nucl. Fusion* **55**, 063031 (2015).
[13] R. L. Neu, S. Brezinsek, M. Beurskens, V. Bobkov, P. de Vries, C. Giroud, E. Joffrin, A. Kallenbach, G. F. Matthews, M.-L. Mayoral et al. *IEEE Trans. Plasma Sci.* **42**, 552 (2014).
[14] P. De Vries, M. Baruzzo, G. Hogeweij, S. Jachmich, E. Joffrin, P. Lomas, G. Matthews, A. Murari, I. Nunes, T. Pütterich et al. *Phys. Plasmas* **21**, 056101 (2014).
[15] E. Fortuna-Zaleśna, J. Grzonka, M. Rasinski, M. Balden, V. Rohde, K. Kurzydlowski et al. *Phys. Scr.* **T159**, 014066 (2014).
[16] E. Fortuna-Zaleśna, A. Weckmann, J. Grzonka, M. Rubel, H. Esser, M. Freisinger, A. Kreter, G. Sergienko and P. Ström *Phys. Scr.* **T167**, 014059 (2016).
[17] E. Fortuna-Zaleśna, J. Grzonka, S. Moon, M. Rubel, P. Petersson, A. Widdowson and Contributors *Phys. Scr.* **T170**, 014038 (2017).
[18] A. Garcia-Carrasco, P. Petersson, M. Rubel, A. Widdowson, E. Fortuna-Zaleśna, S. Jachmich, M. Brix, L. Marot and Contributors, *Nuclear Materials and Energy* **12** 506 (2017).
[19] C. Dickinson, R. D. Davies, J. R. Allison, J. R. Bond, S. Casassus, K. Cleary, R. J. Davis, M. E. Jones, B. S. Mason, S. T. Myers, T. J. Pearson, A. C. S. Readhead, J. L. Sievers, A. C. Taylor, M. Todorovi, G. J. White, and P. N. Wilkinson, *Astrophys. J.* **690**, 1585 (2009).
[20] R. A. Watson, R. Rebolo, J. A. Rubiño-Martín, S. Hildebrandt, C. M. Gutiérrez, S. Fernández-Cerezo, R. J. Hoyland, and E. S. Battistelli, *Astrophys. J.* **624**, L89 (2005).
[21] M. Bacharis, M. Coppins, W. Fundamenski and J. Allen *Plasma Phys. Control. Fusion* **54**, 085010 (2012).
[22] D. Rudakov, A. Litnovsky, W. West, J. Yu, J. Boedo, B. Bray, S. Brezinsek, N. Brooks, M. Fenstermacher, M. Groth et al. *Nucl. Fusion* **49**, 085022 (2009).
[23] S. Krasheninnikov, R. Smirnov and D. Rudakov *Plasma Phys. Control. Fusion* **53**, 083001 (2011).
[24] J. S. Hall *Science* **109**,166 (1949).
[25] W. A. Hiltner *Nature* **163**, 283 (1949).
[26] S. Chandrasekhar and E. Fermi *Astrophys. J.* **118**, 113 (1953).
[27] E. M. Purnell and L. Spitzer, Jr. *Astrophys. J.* **167**, 31 (1971).
[28] B.-G. Andersson, A. Lazarian and J. E. Vaillancourt *Annu. Rev. Astron. Astrophys.* **53**, 501 (2015).
[29] T. Hoang and A. Lazarian *Astrophys. J.* **831**, 159 (2016).
[30] S. J. Barnett *Phys. Rev.* **6**, 239 (1915).
[31] M. Coppins *Phys. Rev. Lett.* **104**, 065003 (2010).
[32] D. Duft, T. Achtzehn, R. Müller, B. A. Huber and T. Leisner, Rayleigh jets from levitated microdroplets, *Nature* **421**, 128 (2003).
[33] J. T. Holgate and M. Coppins, *Phys. Fluids* (in press, 2018).
[34] L. Liao and R. J. Hill *Phys. Rev. Lett.* **119**, 114501 (2017).
[35] S. Chandrasekhar *Proc. Roy. Soc. A* **286**, 1 (1965).
[36] R. A. Brown and L. E. Scriven, The shape and stability of rotating liquid drops, *Proc. R. Soc. Lond. A* **371**, 331 (1980).
[37] O. Ishihara and N. Sato, *IEEE Trans. Plasma Sci.* **29**, 179 (2001).
[38] B. T. Draine and J. C. Weigartner, *Astrophys. J.* **470**, 551 (1996).
[39] S. I. Krasheninnikov, Y. Tomita, R. D. Smirnov, and R. K. Janev, *Phys. Plasmas* **11**, 3141 (2004).
[40] I. H. Hutchinson, *New J. Phys.* **6**, 43 (2004).
[41] S. I. Krasheninnikov, V. I. Shevchenko, and P. K. Shukla, *Phys. Lett. A* **361**, 133 (2007).
[42] S. Krasheninnikov *Phys. Plasmas* **13**, 114502 (2006).
[43] N. Sato *AIP Conf. Proc.* **799**, 97 (2005).
[44] E. S. Dzlieva, M. A. Ermolenko, M. S. Golubev, A. Yu. Ivanov and V. Yu. Karasev *Ukr. J. Phys.* **56**, 1269 (2011).
[45] E. S. Dzlieva, V. Yu. Karasev and O. F. Petrov *J. Exp. Theor. Phys.* **114**, 167 (2012).
[46] G. L. Delzanno and X.-Z. Tang *Phys. Rev. Lett.* **113**, 035002 (2014).
[47] R. Smirnov, T. Soboleva, S. Krasheninnikov and A. Esquivel, 34th EPS Conference on Plasma Physics, Warsaw (2007).
[48] J. Martin, M. Coppins and G. Counsell *J. Nucl. Mater.* **337**, 114 (2005).
[49] F. Militello and W. Fundamenski *Plasma Phys. Control. Fusion* **53**, 095002 (2011).
[50] R. Simonini, G. Corrigan, G. Radford, J. Spence and A. Taroni *Contrib. Plasma Phys.* **34**, 368-373 (1994)